

COORDINATION CONTROL AND ANALYSIS OF TCSC DEVICES TO PROTECT ELECTRICAL POWER SYSTEMS AGAINST DISRUPTIVE DISTURBANCES

Diksha Patel*¹, Parikshit Bajpai*²

*¹M.Tech, SRIT, Jabalpur, India.

*²Assistant Professor, SRIT, Jabalpur, India.

DOI : <https://www.doi.org/10.56726/IRJMETS45376>

ABSTRACT

For protection power grids against disruptive disturbances, we investigate coordination control and the efficient application of thyristor-controlled series compensation (TCSC) in this work. Flexible alternative current transmission systems (FACTS) are components of the electrical grid. The control station, power flow, and phasor measurement units (PMUs) for sensing system states for producing the signals for regulation. We suggest a fresh method for coordination and management of TCSC devices to regulate power flow and adjust branch impedance in the event of unexpected disruptions on branches or buses. Furthermore, a numerical technique is created to calculate the gradient

Keywords: Coordination Control, Thyristor-Controlled Series Compensation (Tcsc), Power Systems, Disruptive Disturbances.

I. INTRODUCTION

Blackouts in the electricity system have grown to be an unsolvable problem for governments and the power sector worldwide in recent decades. To address this problem, some researchers concentrate on finding a method to stop cascading outages in their initial stages [26, 27], others study the impact of communication delay on fault propagation by considering the power grid as a multi-agent system [14, 21], and still others look for disruptive disturbances (also known as triggering events) [22, 28]. Given that many blackouts are started due to the overload precondition [31], it is essential to reduce system stressors brought on by overloads in order to avert catastrophic outcomes and cascading failures.

FACTS devices are used to ensure power oscillation dampening and enhance transient stability in order to reduce system stresses [13]. The reliable running of power grids is made possible by TCSC devices, which control the flow of power [9]. Numerous control strategies have been created thus far, including adaptive neural network backstepping control [17], finite-time H control approach [6], intelligent algorithms [4, 5, 24], and others. Second-order cone programming and model linearization are used to analyse the effect of TCSC in reducing system stress in [2]. Design reliable and nonlinear controllers for TCSC devices as well [11, 32]. The focus of current research is on how to build standalone TCSC controllers or coordinate TCSC with other FACTS, which can both increase the transient stability [16, 18].

It is important to research how TCSC devices work together in practise.

Since multi-agent coordination control has already been widely utilised in other fields [15, 29], it can be used to reduce or even completely eliminate the load placed on the power grid by various events. By Coordination control allows agents to share information with nearby agents. to coordinate separate control operations in order to accomplish the control objective manner. Coordination control of TCSC is achieved by viewing each TCSC device as a smart agent. can be applied to real-time power grid protection [5]. By removing the pressure from having power grids in a methodical manner, it aids in enhancing their resistance to disruptive disturbances [30]. As a result, a coordination control strategy is created in the current efforts to reduce the system stress.

1. Suggest a unique branch control coordination strategy for TCSC devices. coordination-related impedance.
2. Create a practical numerical approach for calculating the gradient vector using cheap expenses for computation.
3. Offer a successful TCSC device deployment plan to lower the number of TCSC without impairing control effectiveness.

The deployment of TCSC takes into account the capacity to deal with unforeseen circumstances, which includes the stress induced by by clogged power flow.

The remaining sections of this essay are organised as follows. Section 2 presents a problem formulation for the coordination control of TCSC devices. The new control method presented in Section 3 of the TCSC. The suggested strategy in Section 4 is validated using IEEE test systems. Section 5 draws the conclusion..

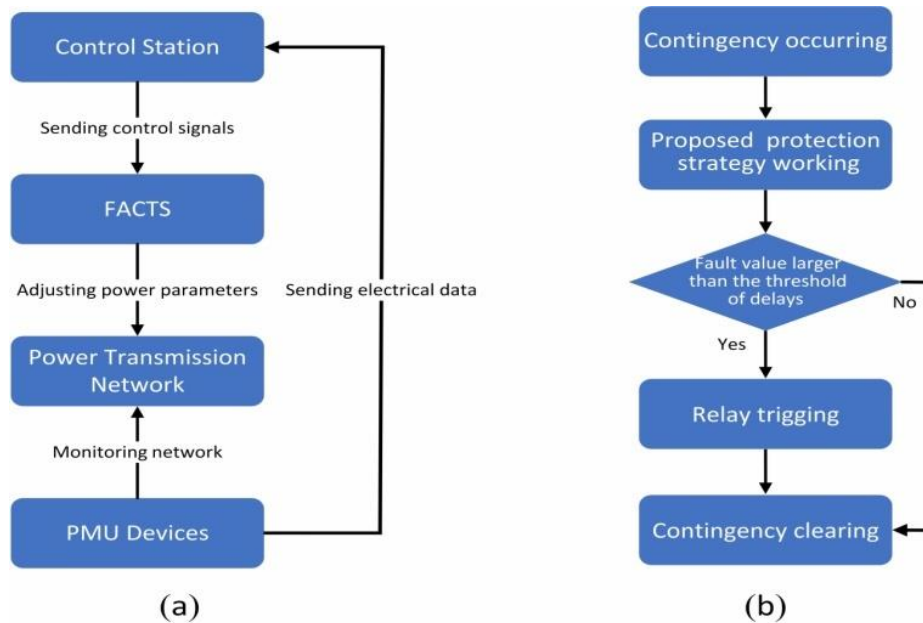


Fig. 1. (a) Smart power grids with PMU and FACTS. (b) Action sequence between the proposed protection strategy and delays

II. PROBLEM FORMULATION

Transmission networks, phase measuring units, FACTS devices, and control stations make up the smart power grid (see Figure 1(a)). PMU is specifically used to detect and transmit real-time state information about buses to the control station. Using the status information, the control station creates appropriate control signals to drive FACTS devices. The impedance of branches is also updated by TCSC devices to control power flow. Refer to [1, 25] to learn how the TCSC, PMU, and control station communicate. The two most used communication protocols for sharing data are synchronous optical networks (Sonet/SDH) and the asynchronous transfer mode (ATM), and electrical utilities have system management choices for handling issues. The cooperation between the suggested protective method and delays is depicted in Figure 1(b). It has been noted that the proposed protection method acts before the relays' protective systems and that it enhances the functionality of the latter. Take into consideration a power grid with n branches without losing generality buses m and. In order to restore the actual power flow P_e to the required values $= (1, 2, \dots, n) C n$ when the power flow on the branch changes, TCSC devices alter the branch impedance. The optimization problem is framed as follows. In order to remove power system stressors, one must develop a control input U for TCSC devices.

$$\min H(\mathbf{Z}) \quad (1)$$

using a tuning parameter of $[0, 1]$, and an objective function $H(\mathbf{Z}) = PR R^2 + PI I^2$. \mathbf{Z} stands for the vector of branch impedance. Keep in mind that PR and PI correspond to P_e 's real and imaginary halves, respectively. Other complicated variables are also affected by the superscripts R and I . The Lyapunov function candidate $V(\mathbf{Z})$ is created below to address Problem 1.

$$V(\mathbf{Z}) = H(\mathbf{Z}) - H(\mathbf{Z}^*),$$

where $H(\mathbf{Z}^*)$ is the minimum value of Problem (1). Then the derivative of $V(\mathbf{Z})$ with respect to the time t gives

$$\frac{dV(\mathbf{Z})}{dt} = \frac{dH(\mathbf{Z})}{dt} = 2(\mathbf{P}_e^R - \sigma^R)^T \frac{d\mathbf{P}_e^R}{dt} + 2\epsilon(\mathbf{P}_e^I - \sigma^I)^T \frac{d\mathbf{P}_e^I}{dt} \quad (2)$$

$$\frac{d\mathbf{P}_e^R}{dt} = \frac{\partial \mathbf{P}_e^R}{\partial \mathbf{Z}^R} \cdot \frac{d\mathbf{Z}^R}{dt} + \frac{\partial \mathbf{P}_e^R}{\partial \mathbf{Z}^I} \cdot \frac{d\mathbf{Z}^I}{dt} \quad (3)$$

$$\frac{d\mathbf{P}_e^I}{dt} = \frac{\partial \mathbf{P}_e^I}{\partial \mathbf{Z}^R} \cdot \frac{d\mathbf{Z}^R}{dt} + \frac{\partial \mathbf{P}_e^I}{\partial \mathbf{Z}^I} \cdot \frac{d\mathbf{Z}^I}{dt} \quad (4)$$

By substituting (3) and (4) into (2)

$$\begin{aligned} \frac{dV(\mathbf{Z})}{dt} &= 2(\mathbf{P}_e^R - \sigma^R)^T \frac{\partial \mathbf{P}_e^R}{\partial \mathbf{Z}^R} \cdot \frac{d\mathbf{Z}^R}{dt} + 2\epsilon(\mathbf{P}_e^I - \sigma^I)^T \frac{\partial \mathbf{P}_e^I}{\partial \mathbf{Z}^R} \cdot \frac{d\mathbf{Z}^R}{dt} \\ &+ 2(\mathbf{P}_e^R - \sigma^R)^T \frac{\partial \mathbf{P}_e^R}{\partial \mathbf{Z}^I} \cdot \frac{d\mathbf{Z}^I}{dt} + 2\epsilon(\mathbf{P}_e^I - \sigma^I)^T \frac{\partial \mathbf{P}_e^I}{\partial \mathbf{Z}^I} \cdot \frac{d\mathbf{Z}^I}{dt} \\ &= 2 \left[\begin{matrix} \mathbf{P}_e^R - \sigma^R \\ \epsilon(\mathbf{P}_e^I - \sigma^I) \end{matrix} \right]^T J(\mathbf{Z}) \left[\begin{matrix} \frac{d\mathbf{Z}^R}{dt} \\ \frac{d\mathbf{Z}^I}{dt} \end{matrix} \right]. \end{aligned} \quad (5)$$

The Jacobian matrix J(Z) in (5)

$$J(\mathbf{Z}) = \begin{bmatrix} \frac{\partial \mathbf{P}_e^R}{\partial \mathbf{Z}^R} & \frac{\partial \mathbf{P}_e^R}{\partial \mathbf{Z}^I} \\ \frac{\partial \mathbf{P}_e^I}{\partial \mathbf{Z}^R} & \frac{\partial \mathbf{P}_e^I}{\partial \mathbf{Z}^I} \end{bmatrix} = (J_{i,j}(\mathbf{Z})) \in R^{2n \times 2n}. \quad (6)$$

The control input U is designed as

$$\mathbf{U} = \begin{bmatrix} \mathbf{U}_R \\ \mathbf{U}_I \end{bmatrix} = \begin{bmatrix} \frac{d\mathbf{Z}^R}{dt} \\ \frac{d\mathbf{Z}^I}{dt} \end{bmatrix}. \quad (7)$$

Because of the intricacy of the system model, obtaining an accurate value of J(Z) is difficult. As a result, a numerical method for estimating J(Z) is proposed. Furthermore, rather than converting the minimization Problem (1) into the KKT condition, this work designs a coordination control approach to minimize the value of H(Z). CCA, rather than the KKT condition, ensures the convergence of the objective function H(Z). Figure 2 depicts a simplified control flow chart for PMUs.

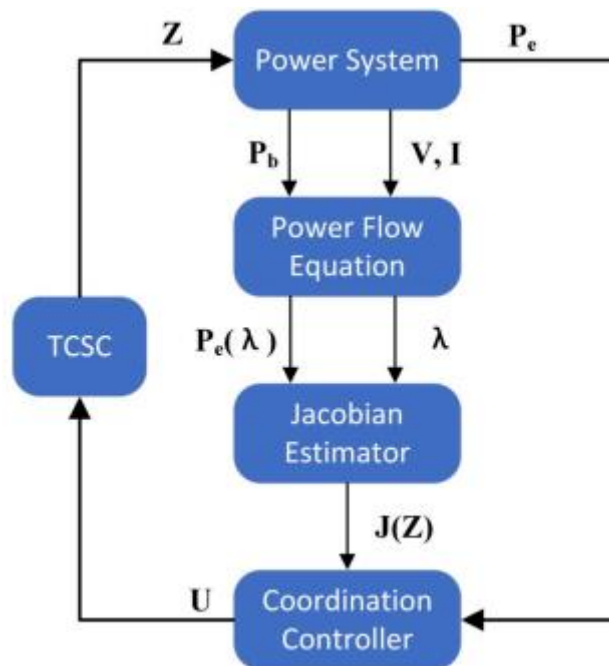


Fig. 2. Regulation signals in smart power grids equipped with TCSC devices.

P_b, V, and I time series should be collected. The Jacobian matrix can then be computed using the power flow equation presented in the appendix by injecting a minor disturbance on the branch. Finally, the controller generates command signals for TCSC devices to regulate power flow in accordance with the defined control law, achieving the optimization goal. It is widely accepted that the TCSC device consists of two primary control blocks, the function of which is to improve the transmission capacity or stability of the power grid [23].

External control can be designed in a variety of ways depending on the control objectives. . The typical PI controller is a sluggish automatic control for power flow regulation [12], and the coordination control presented in this paper is a sort of external control. The internal control block's job is to create adequate gate drive signals for thyristors to generate compensating reactance. Appendix 6.1 shows the link between TCSC impedance and power flow.

Remark 2.1. The purpose of this work is to provide a novel coordination control method for regulating branch impedance via TCSC devices in order to reduce system stress. The proposed method is, in reality, ubiquitous. It is applicable not just to TCSC devices, but also to other FACTS devices.

Remark 2.2. As shown in Appendix 6.2, the generic TCSC model tries to alter branch power flow by varying reactance. The control signal UR merely needs to be set to zero for the control strategy and algorithm established in this study, and control algorithm convergence is still assured.

III. COORDINATION CONTROLLER DESIGN

This section addresses how to determine J(Z) and the creation of coordination control laws.

Generation of feedback control signals

The coordination control law for TCSC devices is given by

$$\mathbf{U} = -\kappa(\mathbf{Z}) \circ J(\mathbf{Z})^T \begin{bmatrix} \mathbf{P}_e^R - \sigma^R \\ \epsilon(\mathbf{P}_e^I - \sigma^I) \end{bmatrix}, \quad (8)$$

$$\kappa_i(\mathbf{Z}) = \begin{cases} c, & Z_i \in [Z_i, \bar{Z}_i]; \\ 0, & \text{otherwise,} \end{cases}$$

with the constant $c > 0$ and the upper limit Z_i and lower limit Z_i . The Coordination Controller (8) is composed of three terms: $\kappa(\mathbf{Z})$, $J(\mathbf{Z})$ and the error vector

$$\Delta \mathbf{P}_e = \begin{bmatrix} \mathbf{P}_e^R - \sigma^R \\ \epsilon(\mathbf{P}_e^I - \sigma^I) \end{bmatrix}.$$

(Z) allows you to alter the branch impedance in a specific interval with upper and lower bounds. J(Z) represents the incremental direction of the goal function in relation to branch impedance. Pe can be calculated by comparing the desired and actual numbers.

Proposition 3.1. The Control Input (8) for TCSC devices can ensure H(Z) convergence.

P r o o f . It is worth noting that both ZR and ZI are changed in accordance with (8). By swapping (7) for (5), we get

$$\frac{dV(\mathbf{Z})}{dt} = 2 \begin{bmatrix} \mathbf{P}_e^R - \sigma^R \\ \epsilon(\mathbf{P}_e^I - \sigma^I) \end{bmatrix}^T J(\mathbf{Z}) \begin{bmatrix} \mathbf{U}_R \\ \mathbf{U}_I \end{bmatrix}. \quad (9)$$

By substituting (8) into (9),

$$\begin{aligned} \frac{dV(\mathbf{Z})}{dt} &= -2 \begin{bmatrix} \mathbf{P}_e^R - \sigma^R \\ \epsilon(\mathbf{P}_e^I - \sigma^I) \end{bmatrix}^T J(\mathbf{Z}) \cdot \kappa(\mathbf{Z}) \circ J(\mathbf{Z})^T \begin{bmatrix} \mathbf{P}_e^R - \sigma^R \\ \epsilon(\mathbf{P}_e^I - \sigma^I) \end{bmatrix} \\ &= -2 \left\| \kappa(\mathbf{Z}) \circ J(\mathbf{Z})^T \begin{bmatrix} \mathbf{P}_e^R - \sigma^R \\ \epsilon(\mathbf{P}_e^I - \sigma^I) \end{bmatrix} \right\|^2 \leq 0 \end{aligned}$$

where $\kappa(\mathbf{Z}) = (\kappa_1(\mathbf{Z}), \kappa_2(\mathbf{Z}), \dots, \kappa_n(\mathbf{Z}))^T$. This indicates that the objective function decreases monotonously as $t \rightarrow +\infty$. Thus, H(Z) is convergent because of $H(\mathbf{Z}) \geq 0$.

Construction of Jacobian estimator

The proposed CCA implementation necessitates the calculation of J(Z). J(Z) is calculated using the linear total least-squares method in [8]. Although there are approximations and relaxations in the modelling of pertinent problems, the procedure remains intricate and needs a considerable number of calculations. As a result, it is critical to devise a numerical method for estimating J(Z) that is computationally light. Four steps are involved in the Jacobian matrix approximation. Pe(Z) is calculated in the first step. The disturbed power flow Pe(ZR + ei) is

then created by injecting a minor disturbance onto each branch, where e_i indicates the unit vector with the i th entry being 1. Taylor's theorem allows PR ($Z^R + e_i$) and PI ($Z^I + e_i$) to be rewritten as

$$P_{e,j}^R(Z^R + \lambda e_i) = P_{e,j}^R(Z) + \lambda \frac{\partial P_{e,j}^R}{\partial Z^R} e_i + O(\lambda) = P_{e,j}^R(Z) + \lambda J_{j,i}(Z) + O(\lambda)$$

and

$$P_{e,j}^I(Z^I + \lambda e_i) = P_{e,j}^I(Z) + \lambda \frac{\partial P_{e,j}^I}{\partial Z^I} e_i + O(\lambda) = P_{e,j}^I(Z) + \lambda J_{j+n,i}(Z) + O(\lambda),$$

respectively. After removing $O(\lambda)$, elements in the i th column of $J(Z)$ are given by

$$J_{j,i}(Z) \approx \frac{P_{e,j}^R(Z^R + \lambda e_i) - P_{e,j}^R(Z)}{\lambda}, \tag{10}$$

$$J_{j+n,i}(Z) \approx \frac{P_{e,j}^I(Z^I + \lambda e_i) - P_{e,j}^I(Z)}{\lambda}. \tag{11}$$

Finally, $Re(Z)$ is restored. Similarly, elements in the $(i + n)$ th column of $J(Z)$ are presented as

$$J_{j,i+n}(Z) \approx \frac{P_{e,j}^R(Z^I + \lambda e_i) - P_{e,j}^R(Z)}{\lambda}, \tag{12}$$

$$J_{j+n,i+n}(Z) \approx \frac{P_{e,j}^I(Z^I + \lambda e_i) - P_{e,j}^I(Z)}{\lambda}. \tag{13}$$

Algorithm 1 Jacobian Estimation Algorithm.

Input: λ and P_b

Output: $J(Z)$

- 1: Set λ and detect P_b
 - 2: Compute $P_e(Z)$
 - 3: **for** $i = 1$ to n **do**
 - 4: $Re(Z) = Re(Z) + \lambda e_i$
 - 5: Compute $P_e(Z^R + \lambda e_i)$
 - 6: Estimate $J_{j,i}(Z)$ with (10) and (11)
 - 7: $Re(Z) = Re(Z) - \lambda e_i$
 - 8: $Im(Z) = Im(Z) + \lambda e_i$
 - 9: Compute $P_e(Z^I + \lambda e_i)$
 - 10: Estimate $J_{j,i+n}(Z)$ with (12) and (13)
 - 11: $Im(Z) = Im(Z) - \lambda e_i$
 - 12: **end for**
-

Algorithm 2 Coordination Control Algorithm.

Input: $s = 0, k = 0, T = 100$ and $S_0 = H_0(Z)$

Output: Z and P_e

- 1: **while** ($H_s(Z) \neq 0$)
 - 2: Detect P_e
 - 3: **if** ($\text{mod}(s, T) = 0$)
 - 4: Update $k = k + 1$
 - 5: Compute S_k
 - 6: **if** ($S_k \geq S_{k-1}$) or ($s = 0$)
 - 7: $S_k \leftarrow S_{k-1}$
 - 8: Detect P_b, V and I
 - 9: Run the JEA for $J(Z)$
 - 10: **end if**
 - 11: **end if**
 - 12: Update Z with (8)
 - 13: Update $s = s + 1$
 - 14: Compute $H_s(Z)$
 - 15: **end while**
-

Algorithm 2 describes the implementation of the suggested coordination controller, which allows for a reduction in the performance index S_k .

Proposition 3.2: CCA for TCSC devices in Algorithm 2 ensures monotonous convergence of S_k .

Proof. CCA allows you to generate a sequence with $S_{k+1} < S_k$ and $S_k > 0, k \in \mathbb{Z}^+$ imply that S_k converges to a constant value $\inf_{k \in \mathbb{Z}^+} S_k$ monotonously as k approaches positive infinity.

Remark 3.1: The final value of S_k is an unknown constant related to power system disruptions. S_k converges to zero when the disturbances are minor. S_k will converge to a constant if the disturbances are substantial and the proposed management approach cannot eliminate them.

IV. CONCLUSION

A novel coordination control technique was developed to reduce system stress by managing power flow using TCSC devices. It also supplied the coordination controller design approach and demonstrated the convergence of the suggested control algorithm. The simulation results for various types of disturbances show that the suggested coordination control strategy has high stability when compared to the traditional control approaches. Finally, modelling findings showed that the successful deployment of TCSCs is closely related to the size of branch impedance, a novel technique to reducing the number of TCSCs.

V. FUTURE WORK

Future work could include optimising the deployment of restricted TCSC agents across the full power network using a distributed control mechanism [7], as well as estimating Jacobian elements from real PMU data without affecting the branch impedance. Furthermore, we intend to develop a multi-state control technique to improve system resilience while taking into account existing delay prevention technologies.

VI. REFERENCES

- [1] M. Begovic, D. Novosel, D. Karlsson, C. Henvill, and G. Michel: Wide-area protection and emergency control. *Proc. T. IEEE* 93 (2005), 876–891. DOI:10.1109/JPROC.2005.847258
- [2] R. Bi, T. Lin, R. Chen, J. Ye, X. Zhou, and X. Xu: Alleviation of post-contingency overloads by SOCP based corrective control considering TCSC and MTDC. *IET Gener. Transmiss. Distr.* 12 (2018), 2155–2164. DOI:10.1049/iet-gtd.2017.1393
- [3] Z. Bie, Y. Lin, G. Li, and F. Li: Battling the extreme: A study on the power system resilience. *Proc. T. IEEE* 105 (2017), 1253–1566. DOI:10.1109/JPROC.2017.2679040
- [4] S. Biswas and K. P. Nayak: A new approach for protecting TCSC compensated transmission lines connected to DFIG-based wind farm. *IEEE Trans. Industr. Inform.* 17 (2021), 5282–5291. DOI:10.1109/TII.2020.3029201
- [5] S. Bruno, G. De, and M. La: Transmission grid control through TCSC dynamic series compensation. *IEEE Trans. Power Syst.* 31 (2016), 3202–3211. DOI:10.1109/TPWRS.2015.2479089
- [6] L. Chang, Y. Liu, Y. Jing, X. Chen, and J. Qiu: Semi-globally practical finite-time H_∞ control of TCSC model of power systems based on dynamic surface control. *IEEE Access.* 8 (2020), 10061–10069. DOI:10.1109/ACCESS.2020.2964265
- [7] Z. Chen and L. Shu: Distributed aggregative optimization with quantized communication. *Kybernetika* 58 (2022), 123–144. DOI:10.1155/2022/3436530
- [8] Y. Chen, J. Wang, A. D. Domínguez-García, and P.W. Sauer: Measurement-based estimation of the power flow Jacobian matrix. *IEEE Trans. Smart Grid* 7 (2015), 2507–2515. DOI:10.1109/TSG.2015.2502484
- [9] T. Duong, J. Yao, and V. Truong: A new method for secured optimal power flow under normal and network contingencies via optimal location of TCSC. *Int. J. Electr. Power Energy Syst.* 52 (2013), 68–80. DOI:10.1016/j.ijepes.2013.03.025
- [10] V. Durković and A. Savić: ATC enhancement using TCSC device regarding uncertainty of realization one of two simultaneous transactions. *Int. J. Electr. Power Energy Syst.* 115 (2020), 105497. DOI:10.1016/j.ijepes.2019.105497
- [11] A. Halder, N. Pal, and D. Mondal: Transient stability analysis of a multimachine power system with TCSC controller – A zero dynamic design approach. *Int. J. Electr. Power Energy Syst.* 97 (2018), 51–71. DOI:10.1016/j.ijepes.2017.10.030
- [12] S. Hameed, B. Das, and V. Pant: A self-tuning fuzzy PI controller for TCSC to improve power system stability. *Electr. Pow. Syst. Res.* 78 (2008), 1726–1735. DOI:10.1016/j.epr.2008.03.005
- [13] R. Hemmati, H. Faraji, and Y. N. Beigvand: Multi objective control scheme on DFIG wind turbine integrated with energy storage system and FACTS devices: Steady-state and transient operation improvement. *Int. J. Electr. Power Energy Syst.* 135 (2022), 107519. DOI:10.1016/j.ijepes.2021.107519
- [14] J. Hu: On Robust Consensus of Multi-Agent Systems with Communication Delays Volume. *Kybernetika* 45 (2009), 768–784.

- [15] J. Hu, G. Chen, and H. Li: Distributed event-triggered tracking control of leader-follower multi-agent systems with communication delays. *Kybernetika* 47 (2011), 630–643.
- [16] Y. Liu, Q. Wu, and X. Zhou: Coordinated switching controllers for transient stability of multi-machine power systems. *IEEE Trans. Power Syst.* 31 (2016), 3937–3949. DOI:10.1109/TPWRS.2015.2495159
- [17] Y. Luo, S. Zhao, D. Yang, and H. Zhang: A new robust adaptive neural network back stepping control for single machine infinite power system with TCSC. *IEEE/CAA J. Automat. Sinica* 7 (2020), 48–56. DOI:10.1109/JAS.2019.1911798
- [18] H. Kumar and P. Singh: Coordinated control of TCSC and UPFC to aid damping oscillations in the power system. *Int. J. Electron.* 106 (2019), 1938–1963. DOI:10.1080/00207217.2019.1636296
- [19] T. Nguyen and F. Mohammadi: Optimal placement of TCSC for congestion management and power loss reduction using multi-objective genetic algorithm. *Sustainability* 12 (2020), 2813. DOI:10.3390/su12072813
- [20] M. Panteli and P. Mancarella: The grid: Stronger, bigger, smarter?: Presenting a conceptual framework of power system resilience. *IEEE Pow. Energy Mag.* 13 (2015), 58–66. DOI:10.1109/MPE.2015.2397334
- [21] T. Prakash, P. V. Singh, and S. R. Mohanty: A synchrophasor measurement based wide-area power system stabilizer design for inter-area oscillation damping considering variable time-delays. *Int. J. Electr Power Energy Syst.* 105 (2019), 131–141. DOI:10.1016/j.ijepes.2018.08.014
- [22] R. Rocchetta and E. Patelli: Assessment of power grid vulnerabilities accounting for stochastic loads and model imprecision. *Int. J. Electr. Power Energy Syst.* 98 (2018), 219–232. DOI:10.1016/j.ijepes.2017.11.047
- [23] A. Rosso, C. A. Canizares and V. M. Dona: A study of TCSC controller design for power system stability improvement. *IEEE Trans. Power Syst.* 18 (2003), 1487–1496. DOI:10.1109/TPWRS.2003.818703
- [24] B. Shafik, H. Chen, I. Rashed, and A. Sehiemy: Adaptive multi objective parallel seeker optimization algorithm for incorporating TCSC devices into optimal power flow framework. *IEEE Access.* 7 (2019), 36934–36947. DOI:10.1109/ACCESS.2019.2905266
- [25] V. Terzija, G. Valverde, D. Cai, P. Regulski, V. Madani, J. Fitch, S. Skok, M. Begovic, and A. Phadke: Wide-area monitoring, protection, and control of future electric power networks. *Proc. T. IEEE* 99 (2011), 80–93. DOI:10.1109/JPROC.2010.2060450
- [26] J. Xu, R. Yao and F. Qiu: Mitigating cascading outages in severe weather using simulation-based optimization. *IEEE Trans. Power Syst.* 39 (2021), 204–213. DOI:10.1109/tpwrs.2020.3008428
- [27] C. Zhai, G. Xiao, M. Meng, H. Zhang, and B. Li: Identification of catastrophic cascading failures in protected power grids using optimal control. *J. Energ. Engrg.* 147 (2021), 6020001. DOI:10.1061/(ASCE)EY.1943-7897.0000731
- [28] C. Zhai, G. Xiao, H. Zhang, P. Wang, and T. Pan: Identifying disruptive contingencies for catastrophic cascading failures in power systems. *Int. J. Electr. Power Energy Syst.* 123 (2020), 106214. DOI:10.1016/j.ijepes.2020.106214
- [29] C. Zhai and Y. Hong: Decentralized sweep coverage algorithm for multiagent systems with workload uncertainties. *Automatica* 49 (2013), 2154–2159. DOI:10.1016/j.automatica.2013.03.017
- [30] C. Zhai, G. Xiao, H. Zhang and T. Pan: Cooperative control of TCSC to relieve the stress of cyber-physical power system. In: *International Conference on Control, Automation, Robotics and Vision 2018*, pp. 4849–4854. DOI:10.1186/s13662-018-1910-6
- [31] C. Zhai, H. Zhang, G. Xiao, and T. Pan: A model predictive approach to protect power systems against cascading blackouts. *Int. J. Electr. Power Energy Syst.* 113 (2019), 310– 321. DOI:10.1016/j.ijepes.2019.05.029
- [32] C. Zhang, X. Wang, Z. Ming, Z. Cai, and H. Linh: Enhanced nonlinear robust control for TCSC in power system. *Math. Probl. Eng.* 2018 (2018), 1416059. DOI:10.1155/2018/3495096